

To appear in *The Astrophysical Journal*, Vol. 481, June 1, 1997

Low Surface Brightness Galaxies in the Local Universe. III. Implications for the Field Galaxy Luminosity Function

D. Sprayberry

Kapteyn Laboratorium, University of Groningen, Postbus 800,
9700 AV Groningen, The Netherlands
Email: dspray@astro.rug.nl

C. D. Impey

Steward Observatory, University of Arizona, Tucson, AZ 85721
Email: cimpey@as.arizona.edu

M. J. Irwin

Royal Greenwich Observatory, Madingley Road, Cambridge, UK CB3 0EZ
Email: mike@mail.ast.cam.ac.uk

and

G. D. Bothun

Department of Physics, University of Oregon, Eugene, OR 97403
Email: nuts@moo.uoregon.edu

ABSTRACT

We present a luminosity function for low surface brightness (LSB) galaxies identified in the APM survey of Impey et al. (1996). These galaxies have central surface brightnesses ($\mu(0)$) in B in the range $22.0 \leq \mu(0) \leq 25.0$. Using standard maximum-likelihood estimators, we determine that the best-fit Schechter function parameters for this luminosity function (LF) are $\alpha = -1.42$, $M^* = -18.34$, and $\phi^* = 0.0036$, assuming $H_0 = 100 h_{100} \text{ km s}^{-1} \text{ Mpc}^{-1}$. We compare the luminosity and number densities derived from this luminosity function to those obtained from other recent field galaxy studies and find that surveys which do not take account of the observation selection bias imposed by surface brightness are missing a substantial fraction of the galaxies in the local universe. Under our most conservative estimates, our derivation of the LF for LSB galaxies suggests that the CfA redshift survey has missed at least one third of the local galaxy population. This overlooked fraction is not enough by itself to explain the large number of faint blue galaxies observed at moderate redshift under no-evolution models, but it does help close the gap between local and moderate-redshift galaxy counts.

1 Introduction

The optical luminosity function (LF) of galaxies is one of the fundamental building blocks of cosmology. Accurate knowledge of the luminosity function is necessary for, among other things, estimating the mean luminosity density of the universe, and predicting the redshift distribution of objects in various magnitude intervals (see e.g., the review by Binggeli et al. 1988). The shape of the luminosity function also provides an important test for theories of galaxy formation (e.g., Press & Schechter 1974). Further, considerable attention has been focussed of late on the large numbers of blue galaxies found in deep surveys, first described by Kron (1980) and Hall & Mackay (1984). The degree to which number counts of these galaxies exceed those predicted from local observations (e.g., Bruzual & Kron 1980 and Guiderdoni & Rocca-Volmerange 1990), and indeed whether an excess exists at all (compare Koo et al. 1993 and McGaugh 1994), depend on the shape, normalization and color dependence of the luminosity function.

One of the problems with building a galaxy luminosity function is that surveys are limited in the detection of diffuse galaxies by the brightness of the night sky, and in the detection of compact galaxies by the difficulty in distinguishing stars and galaxies. As Disney (1976) and Disney & Phillipps (1983) have demonstrated, at a given luminosity a survey will identify preferentially those galaxies that have the maximum possible angular size above the limiting isophote. At a constant luminosity, galaxies of high surface brightness (HSB) become indistinguishable from stars, and galaxies of low surface brightness (LSB) fall below the limiting isophote over most of their extent. Although they purport to be magnitude limited, galaxy surveys which do not take account of surface brightness effects are missing an unknown but potentially large number of galaxies in each magnitude bin. Recent surveys of the Virgo cluster by Impey et al. (1988) and of the Fornax cluster by Irwin et al. (1990) and Bothun et al. (1991) have taken account of this potential source of bias by deliberately searching for LSB galaxies. They have found that previous surveys missed a significant fraction of the cluster populations, particularly at fainter luminosities ($M_B \gtrsim -16$), and Impey et al. (1988) determined that inclusion of LSB galaxies in Virgo steepened the low-luminosity tail of that cluster's luminosity function considerably. To date, however, no estimates of the field galaxy luminosity function have addressed the effects of surface brightness bias. However, McGaugh et al. (1995a) found that the space density of galaxies as a function of central surface brightness appears to be flat below $\mu_B(0) = 22.0$. Also, Sprayberry et al. (1996) found a space density of galaxies as a function of central surface brightness that appeared flat below $\mu_B(0) = 23.0$ after descending from a peak around $\mu_B(0) = 21.75$. Although many of these LSB galaxies are not necessarily faint, the forms of these distribution functions strongly suggest that the normalization of the galaxy space density at $z = 0$ has been strongly influenced by surface brightness selection effects.

We have recently completed a survey for LSB galaxies in the region defined by $-3^\circ \leq \delta \leq 3^\circ$ and $|b| > 30^\circ$, surveying about 786 square degrees of sky with the Automated

Plate Measuring (APM) system at Cambridge.¹ We have identified 693 galaxies, most previously uncataloged and most with central surface brightness $\mu_B(0) > 22$ mag arcsec⁻². The complete catalog of this survey appears in Impey et al. (1996) (Paper I). The selection effects and completeness corrections for the survey are analyzed in detail in Sprayberry et al. (1996) (Paper II).

In this paper, we present the luminosity function for LSB galaxies from the APM survey and compare that luminosity function to those obtained from the CfA redshift survey. We also review suggestions by Phillipps et al. (1990), McGaugh (1994), McLeod (1994), and Ferguson & McGaugh (1995) that LSB galaxies might account at least partially for the large numbers of faint blue galaxies seen in deep surveys. Section 2 describes the survey data and presents the samples used for determining the luminosity function and the corrections applied to those samples. Section 3 covers the methods used to develop the luminosity functions. Section 4 presents the luminosity functions and compares the results to those obtained from the CfA redshift survey. Section 5 reviews the consequences of this LSB luminosity function for the general field luminosity function and for the question of local counterparts to the faint blue galaxies. Finally, Section 6 summarizes our conclusions. Throughout this paper, we assume $H_0 = 100 h_{100} \text{ km s}^{-1} \text{ Mpc}^{-1}$. Also, all magnitudes and surface brightnesses used here are in the Johnson B band.

2 Samples Used

The APM survey for LSB galaxies is presented in Paper I, and Paper II describes the details of how LSB galaxies were identified and calibrated. Paper II also presents a selection function that gives the completeness of the survey as a function of galaxy central surface brightness and scale length (hereafter, “the APM selection function”).

We conducted followup optical spectroscopy at the Multiple Mirror Telescope² and 21 cm H I spectroscopy at Arecibo Observatory³ to obtain radial velocities for as many of the galaxies as possible. To date we have measured recessional velocities for 332 of the 693 galaxies on the list, of which 190 come from H I spectroscopy and 142 from optical spectroscopy. These heliocentric velocities are presented in Paper I. For developing the luminosity function, we have further corrected these heliocentric velocities to the rest frame of the Local Group, using the standard correction $v_{corr} = v_{hel} + 300 \sin l \cos b$. No correction was applied for Virgocentric infall since the median velocity of the sample places most of

¹The APM is a National Astronomy Facility, at the Institute of Astronomy, operated by the Royal Greenwich Observatory. A general description of the APM facility is given by Kibblewhite et al. (1984).

²The Multiple Mirror Telescope is a facility jointly operated by the Smithsonian Institution and the University of Arizona.

³The Arecibo Observatory is part of the National Astronomy and Ionosphere Center. The NAIC is operated by Cornell University under a cooperative agreement with the National Science Foundation.

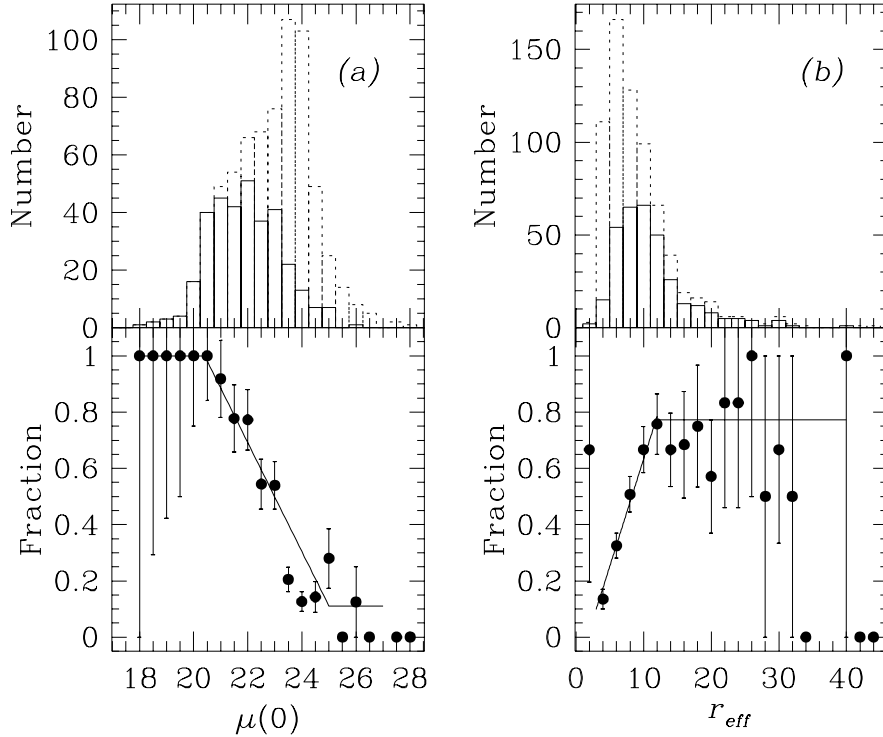


Figure 1: Structural properties of the complete LSB sample and the subset with radial velocities. (a) shows the distribution as a function of B central surface brightness, and (b) shows the distribution as a function of half-light radius. In the upper panels, the dotted histogram is the distribution of the complete sample, and the solid histogram is the distribution of the subset with velocities. In the lower panels, the filled circles show the fraction of galaxies with velocities for each bin, with error bars from counting statistics. The solid lines show the parametrizations described in the text.

the galaxies well beyond the Local Supercluster. These corrected velocities were then used to estimate distance moduli using the relation:

$$m - M = 5 [\log v_{corr} - \log H_0 + 5] \quad (1)$$

assuming as noted above that $H_0 = 100 h_{100} \text{ km s}^{-1} \text{ Mpc}^{-1}$.

The galaxies with velocities do not form a random subset of the overall survey. For reasons of observational efficiency, like all other galaxy surveyors we favored galaxies of higher central surface brightness and larger angular size. Figure 1 shows the distributions of central surface brightness and half-light radius for the complete sample and for the subset with velocities, along with the ratios of the two sets by bin. We assume that the galaxies for which we have measured redshifts are representative of all galaxies in a given bin of surface brightness and angular size. This additional source of bias must be taken into account in preparing a luminosity function. We have parameterized this bias in the simple

forms depicted in Figure 1: three separate linear fits in the different regions of the $\mu(0)$ distribution

$$p_\mu = \begin{cases} 1.000, & \mu(0) < 20.25 \\ 4.950 - 0.194 \mu(0), & 20.25 \leq \mu(0) \leq 25.0 \\ 0.111, & \mu(0) > 25.0 \end{cases} \quad (2)$$

where $\mu(0)$ is in mag arcsec⁻², and in the different regions of the half-light radius distribution

$$p_{r_e} = \begin{cases} 0.667, & r_{eff} < 3 \\ -0.130 + 0.076 r_{eff}, & 3 \leq r_{eff} \leq 13 \\ 0.773, & r_{eff} > 13 \end{cases} \quad (3)$$

where r_{eff} is in arcseconds. The final probability that an LSB galaxy will be detected by the APM and included in the subset with velocities is given by

$$p_{tot} = p_{APM} \times p_\mu \times p_{r_e} \quad (4)$$

where p_{APM} is the probability derived from the APM selection function of Paper II. Equation 4 assumes that the corrections in $\mu(0)$ and r_{eff} are separable. This assumption is reasonable for our sample, because $\mu(0)$ and r_{eff} are uncorrelated: Pearson's $r = 0.075$ and the Spearman rank correlation coefficient $s = -0.121$, and neither coefficient is significantly different from zero.

We note that Figure 1 shows that the surface brightness range $23.5 \leq \mu(0) \leq 24.5$ includes a large number of identified galaxies, but that a very small fraction of those galaxies were observed spectroscopically. Also, the observed fraction as a function of angular size declines sharply at small sizes. These features are artifacts of the two stages in which the APM survey was performed. The first stage identified LSB galaxies of large angular size, and all the followup spectroscopy was performed on galaxies in this first list. The second stage identified small angular size galaxies, which also tended to be predominantly in the surface brightness range $23.5 \leq \mu(0) \leq 24.5$. The interested reader is referred to Paper II for a more complete discussion of the survey mechanics. Here we note only that the actual observed fraction in the range $23.5 \leq \mu(0) \leq 24.5$ lies *below* the parametrization of Equation 2, which implies that the parametrized correction is too small for those two surface brightness bins. Any bias introduced by this effect is “conservative”, in that it will result in an underestimation of the total number of LSB galaxies.

We can estimate the completeness of our sample of galaxies using the $\langle V/V_{max} \rangle$ test of Schmidt (1968). For the complete set of 693 galaxies identified by the APM, the test yields $\langle V/V_{max} \rangle = 0.15 \pm 0.04$ with no corrections for incompleteness, and $\langle V/V_{max} \rangle = 0.44 \pm 0.06$ after correcting for incompleteness using the APM selection function described in Paper II. For the subset of 332 galaxies with velocities, the test gives $\langle V/V_{max} \rangle = 0.04 \pm 0.05$ with no corrections for incompleteness, $\langle V/V_{max} \rangle = 0.34 \pm 0.07$ after applying just the APM selection function, and $\langle V/V_{max} \rangle = 0.50 \pm 0.07$ after applying the APM selection function and the further correction for incompleteness in the velocity observations from Equations 2, 3, and 4

(as depicted in Figure 1). The corrections thus substantially remove the incompleteness in both the complete set and in the subset chosen for spectroscopy.

There is yet another source of bias to be found in the magnitudes measured for LSB galaxies. The magnitudes measured in our survey are isophotal magnitudes, not extrapolated or asymptotic. The median limiting isophote is $\mu_{lim} \approx 27.4$ mag arcsec⁻². As authors from Disney (1976) to McGaugh (1994) have pointed out, use of isophotal magnitudes will cause galaxy luminosities to be underestimated, and the underestimation becomes more severe with decreasing central surface brightness. Most LSB galaxies are well-described by exponential surface brightness profiles (Impey et al. 1988, Bothun et al. 1991, and McGaugh & Bothun 1994) of the form

$$\mu(r) = \mu(0) + 1.086 \frac{r}{l} \quad (5)$$

where $\mu(0)$ is the central surface brightness in mag arcsec⁻² and l is the exponential scale length in arcseconds. This simple analytical form allows a direct calculation of the ratio of the total galaxy flux to that observed within the limiting isophote, as

$$\frac{F_{obs}}{F_{tot}} = 1 - (1 + n_l)e^{-n_l} \quad (6)$$

where n_l is the number of scale lengths l observed within the limiting isophote. This simple approximation will clearly understate the ratio for galaxies with central condensations, such as spirals with bulges. The isophotal aperture in units of the galaxy scale length is then given by

$$n_l = \frac{\mu_{lim} - \mu(0) - 10 \log(1 + z) - k(z)}{1.086} \quad (7)$$

where μ_{lim} is the surface brightness of the limiting isophote. The first term involving z accounts for the $(1 + z)^4$ cosmological dimming in surface brightness, and the second corrects for the redshifting of the galaxy's spectral energy distribution (the k correction). The k correction of course depends on galaxy type as well as redshift. The magnitudes and surface brightness for the LSB galaxies with velocities have been corrected as described in Paper II using the tabulated k corrections of Coleman et al. (1980). The $B - V$ and $V - R$ colors for galaxy types Sbc, Scd, and Irr closely match the range of colors observed among the galaxies for which we obtained CCD photometry. The absolute magnitudes have been corrected according to Equations 7 and 6, so as to avoid skewing the luminosity function by this tendency to underestimate galaxy luminosities.

Of course, our set of LSB galaxies is not itself a fair sample of the local galaxy population, precisely because it excludes most galaxies with $\mu(0) \lesssim 22$ mag arcsec⁻². However, it is still useful to derive a luminosity function for this set, so that this LF can be compared to one derived from higher surface brightness galaxies. In this way, it is possible to obtain some idea of how surface brightness selection effects have influenced estimates of the density of local galaxies (see also McGaugh et al. 1995 and Paper II). To validate such a comparison, it is necessary first to compare the range of surface brightnesses covered by the present set

of LSB galaxies with the range covered by other surveys. Unfortunately, no other recent galaxy redshift surveys have published surface brightness data for their galaxies. Thanks to the recent release of a digitized version of the original Palomar Observatory Sky Survey (the Digitized Sky Survey⁴ or DSS), it is now possible to make independent measurements of the basic photometric parameters of any object visible on the original survey, when the celestial coordinates of the surveyed galaxies are known. The CfA Redshift Survey described by e.g., Marzke et al. (1994b) is based on Zwicky’s Catalog of Galaxies and Clusters of Galaxies, which was in turn created by visual examination of the Palomar Observatory Sky Survey plates, so every object included in that survey should be visible on the DSS. Most importantly, the coordinates of galaxies surveyed by the CfA are publicly available, so that it is possible to retrieve images of the surveyed galaxies from the DSS. Thus it should be possible to measure the surface brightness range covered by the CfA Redshift survey. The lack of publicly available coordinates prevents us from making a similar analysis of other recent redshift surveys.

We recovered from the Astrophysics Data System listing of the CfA Redshift Survey the coordinates of every galaxy listed in the regions of sky used by Marzke et al. (1994b). We subdivided that list according to the morphological categories used by Marzke et al. (1994a), and we randomly selected 10% of the galaxies within each morphological class to keep the number of galaxies manageable. This selection yielded a list of 579 galaxies. We then retrieved images from the DSS of this randomly chosen subset and analyzed the images using the same algorithms used in our APM LSB galaxy survey. In this way, we obtained extrapolated central surface brightnesses for the CfA galaxies that are directly comparable to those obtained in the course of the APM survey. Paper II contains a complete description of the process of estimating the extrapolated central surface brightness. As a check on the calibrations, we also retrieved from the DSS images of a randomly chosen subset of the APM LSB galaxies and analyzed them. After cross-calibration, the results for the APM LSB galaxies were consistent with those obtained from the deeper UKST plate materials used in the APM LSB survey, with the exception that the lowest surface brightness objects were not visible on the DSS.

The surface brightness distribution for the CfA Redshift survey is shown in the upper panel of Figure 2. The solidly drawn smooth curve represents the best Gaussian fit to the CfA distribution. The lower panel shows the complete SB distribution obtained by the APM for one UKST field. Also drawn for illustration in each panel is a dashed curve representing the canonical “Freeman Law”, a Gaussian centered at $\mu(0) = 21.65$ with $\sigma = 0.35$ (Freeman 1970). It is clear from Figure 2 that the range of surface brightnesses covered by the CfA Redshift Survey is very narrow, narrower even than the “Freeman Law.”

⁴Based on photographic data of the National Geographic Society – Palomar Observatory Sky Survey (NGS-POSS) obtained using the Oschin Telescope on Palomar Mountain. The NGS-POSS was funded by a grant from the National Geographic Society to the California Institute of Technology. The plates were processed into the present compressed digital form with their permission. The Digitized Sky Survey was produced at the Space Telescope Science Institute under US Government grant NAG W-2166.

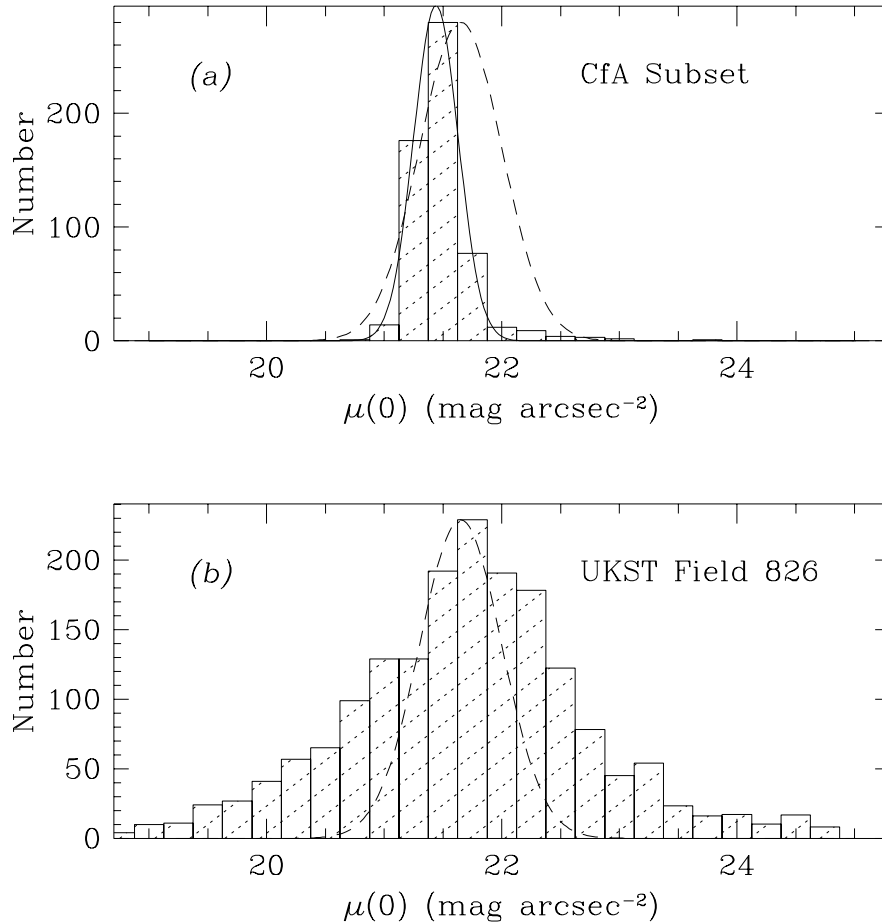


Figure 2: Distributions of central surface brightness for (a) a randomly chosen sample of galaxies from the CfA redshift survey, and (b) the complete list of galaxies identified by machine scan of one UKST survey field. In (a) the solid curve represents the best fit of a Gaussian to the CfA survey surface brightness distribution. In both panels the dashed Gaussians illustrate the canonical “Freeman Law” of $\mu(0) = 21.65 \pm 0.35$. The distribution in (b) is corrected for incompleteness of the detection algorithm for $\mu_B(0) \lesssim 25$ as described in Paper II.

The best-fit Gaussian to the CfA distribution has a center at $\mu(0) = 21.44$ and $\sigma = 0.19$. This is completely consistent with the investigation of the Zwicky magnitude scale by Bothun & Cornell (1990) who find that this magnitude is not a sky-limited magnitude. In this case, one expects surface brightness effects to completely dominate the magnitude estimates. In essence, the Zwicky magnitude is very much a “bulge” or high surface brightness magnitude and is insensitive to extended, low surface brightness light. In contrast, the APM LSB survey has identified galaxies over a much broader range, as described in Paper II. Clearly, the identification of galaxies for the CfA Redshift survey suffered from a substantial bias against LSB galaxies. In all the following analysis, we use only those galaxies from the APM

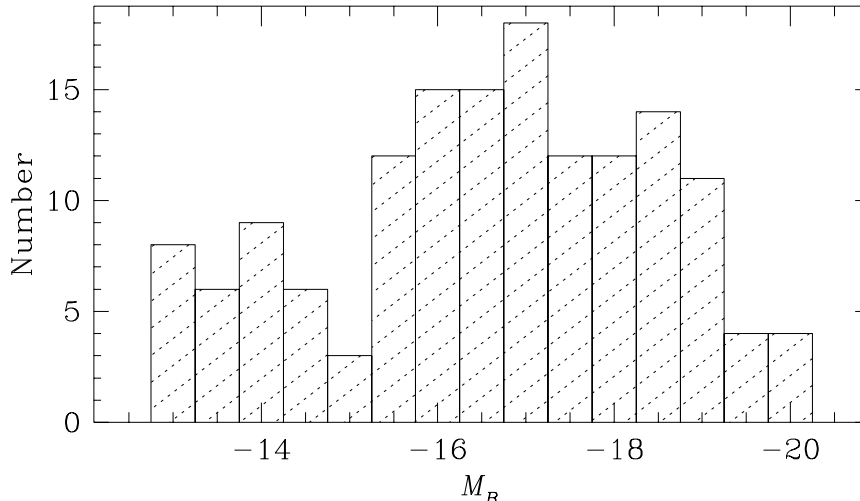


Figure 3: Distribution of absolute magnitudes for the LSB galaxies ($\mu(0) > 22.0$ mag arcsec $^{-2}$) used to develop the LF. This distribution includes the effects of the correction from isophotal to total magnitudes described in Equations 7 and 6.

LSB survey with $\mu(0) > 22.0$ mag arcsec $^{-2}$, or 3σ fainter than the typical value found in the CfA Survey. This limitation assures that the resulting LF covers a different regime of surface brightness parameter space from that covered by the LFs of Marzke et al. (1994b) and Marzke et al. (1994a). We note that there is a weak LSB tail in the CfA distribution: the overall χ^2_ν of the Gaussian fit is 1.37, virtually all of which is due to this tail. However, the very weakness of this tail, when compared to the APM distribution in the lower panel, underscores the severity of the SB selection bias inherent in the CfA survey. We note also that the CfA survey does not identify nearly as many high surface brightness galaxies as does the APM. This lack is most likely due to the general absence of galaxies smaller than 1 arcminute from the Zwicky catalog; many of the high surface brightness galaxies identified by the APM are smaller than 1 arcminute. Figure 3 shows the distribution of absolute magnitudes for the LSB survey galaxies with $\mu(0) > 22.0$ mag arcsec $^{-2}$.

3 Methods

The differential luminosity function of field galaxies $\phi(M)dM$ is defined as the function giving, at each absolute magnitude M , the number of galaxies per Mpc $^{-3}$ in the luminosity interval $M + dM/2 \leq M \leq M - dM/2$. Because the area surveyed by the APM LSB survey covers a wide area of sky and cuts across several large scale structures, we adopt two density-independent techniques for estimating the LF. The first is the parametric maximum likelihood technique developed by Sandage et al. (1979) (hereafter STY). The second is the stepwise maximum likelihood method (hereafter SWML) developed by Efstathiou et al.

(1988). Both methods assume that the LF has a universal form, independent of position, allowing the probability of a galaxy’s inclusion in a complete catalog to be written simply in terms of the LF itself. The STY method is continuous and uses all the galaxy data, but it requires the assumption of a parametrized form for the LF. It therefore gives no information as to the suitability of the parametrized form chosen to represent the LF. The SWML method requires binning the data, but it requires no assumptions about the shape of the LF. It can therefore be used in combination with the STY method to provide an independent check on the goodness-of-fit of the chosen parametrization, as described by Efstathiou et al. (1988). Like Marzke et al. (1994a) and virtually all others who have used this combination of methods, we assume in the STY method a luminosity function parameterization in the form first proposed by Schechter (1976), which is written in absolute magnitudes as

$$\phi(M)dM = 0.4 \ln 10 \phi_* \left[(10^{0.4(M_*-M)})^{1+\alpha} e^{-(10^{0.4(M_*-M)})} \right] dM \quad (8)$$

Using the two methods together thus gives best-fit values for the Schechter function parameters α (the faint-end slope) and M^* (the characteristic absolute magnitude of the “knee”), as well as a probability that the underlying galaxy population is well-described by the best-fit Schechter function.

There is one major difficulty with applying these methods to the APM LSB galaxy survey data. Both the STY method and the SWML method assume that the galaxy catalog in use is magnitude limited, or that all galaxies with $m < m_{lim}$ have the same probability ($p < 1$) of being included in the catalog, as in the case of a redshift survey that uniformly samples a magnitude-limited catalog with $1/n$ sampling. In our case, however, each galaxy has a unique probability of inclusion that is determined from Equation 4, so the given forms of the STY and SWML methods require modification. Zucca et al. (1994) recently addressed this problem. They derived a simple modification to the STY estimator that accounts for the unique observation probability assigned to each galaxy:

$$\mathcal{L} = \prod_{i=1}^N p_i^{w_i} \quad (9)$$

where \mathcal{L} is the likelihood to be maximized, the weight w_i is defined as the inverse of the probability that the i th galaxy will be included in the sample (i.e., for our situation $w_i = 1/p_{tot,i}$, with $p_{tot,i}$ from Equation 4), and p_i is as defined by STY:

$$p_i = \phi(M_i) \left/ \int_{M_{max}(z_i)}^{-\infty} \phi(M)dM \right. \quad (10)$$

The corresponding change to the SWML estimator of Efstathiou et al. (1988) immediately yields:

$$\ln \mathcal{L} = \sum_{i=1}^N W(M_i - M_k) w_i \ln \phi_k - \sum_{i=1}^N w_i \ln \left\{ \sum_{j=1}^{N_p} \phi_j \Delta MH (M_{max}(z_i) - M_j) \right\} + \text{const} \quad (11)$$

where the ϕ_k are the luminosity function values within each bin, N is the total number of galaxies in the sample, N_p is the number of steps, $M_{max(z_i)}$ is the maximum (i.e., the faintest) absolute magnitude visible at z_i , ΔM is the bin width in magnitudes, and the window functions are

$$W(x) = \begin{cases} 1, & |x| \leq \Delta M/2 \\ 0, & \text{otherwise} \end{cases} \quad (12)$$

and

$$H(x) = \begin{cases} 0, & x < -\Delta M/2 \\ (x/\Delta M + 1/2), & |x| \leq \Delta M/2 \\ 1, & x > \Delta M/2 \end{cases} \quad (13)$$

There is an implied sum over the doubled index k in the first term of Equation 11.

Finally, the survey biases must also be incorporated into the normalization. Both the STY and SWML estimators are normalized in the manner described by Efstathiou et al. (1988) using the unbiased minimum variance estimate of the mean density as developed by Davis & Huchra (1982), but with a modification to the estimator to incorporate the corrections for survey incompleteness. This normalization proceeds in three steps. First, a selection function is defined as

$$S(x) = \int_{max[M_{max(x), M_2}]^{M_1}} \phi(M) dM \bigg/ \int_{M_2}^{M_1} \phi(M) dM \quad (14)$$

for galaxies in the range $M_1 < M < M_2$, where $M_{max(x)}$ is the maximum (i.e., the faintest) absolute magnitude visible at distance x according to the catalog limits. Second, this selection function is then corrected to incorporate the incompleteness correction, so that it includes the combined probability of detecting and spectroscopically observing an LSB galaxy in our survey:

$$S_{tot}(x_i) = S(x_i) \times p_{tot,i} \quad (15)$$

where $p_{tot,i}$ is obtained from 4. Finally, the mean density of galaxies is obtained from the corrected selection function as described by Efstathiou et al. (1988):

$$\langle n \rangle = \frac{1}{V} \sum_{i=1}^N \frac{1}{S_{tot}(x_i)} \quad (16)$$

where the sum extends over all the galaxies in volume V . The mean density is converted to a Schechter function normalization as:

$$\phi_* = \frac{\langle n \rangle}{\Gamma(\alpha + 1, 10^{0.4(M_* - M_2)}) - \Gamma(\alpha + 1, 10^{0.4(M_* - M_1)})} \quad (17)$$

where Γ is the Euler incomplete gamma function.

Zucca et al. (1994) also estimated the effects of failing to consider the individual galaxy weights. Their simulations revealed that use of Equation 10 to determine the Schechter

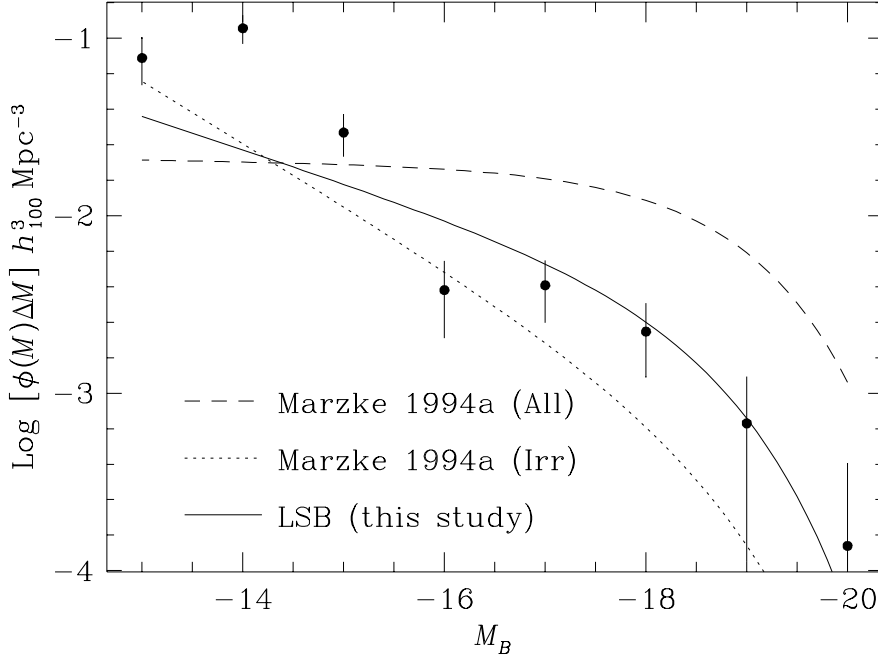


Figure 4: Luminosity function for LSB galaxies from the APM survey. The solid line represents the maximum likelihood Schechter function, and the points with error bars represent the model-independent step-wise maximum likelihood function. Note that for the LSB galaxies, the model-independent binned LF shows a significant excess of low luminosity galaxies, beyond the level of the maximum likelihood Schechter function. The dashed line shows the maximum likelihood Schechter function estimated by Marzke et al. (1994a) for all morphological types in the CfA redshift survey, and the dotted line shows the maximum likelihood Schechter function estimated by Marzke et al. for irregulars in the CfA redshift survey

function parameters for a galaxy sample with significant incompleteness ($\langle V/V_{max} \rangle \lesssim 0.3$) would bias the results towards flatter faint-end slopes (i.e., lower absolute values of α) and brighter values of M_* . We can objectively determine individual galaxy weights from parameters of our survey technique (the APM selection function) and from the internal statistics of our followup observations (Figure 1 and Equations 2 and 3), so Equations 9 and 11 are the clear techniques of choice for our data.

4 Results

Figure 4 shows the luminosity function for the LSB galaxies ($\mu(0) \geq 22.0$) from the APM survey. The solid line represents the maximum likelihood Schechter function from the STY method, and the points with error bars represent the model-independent SWML method.

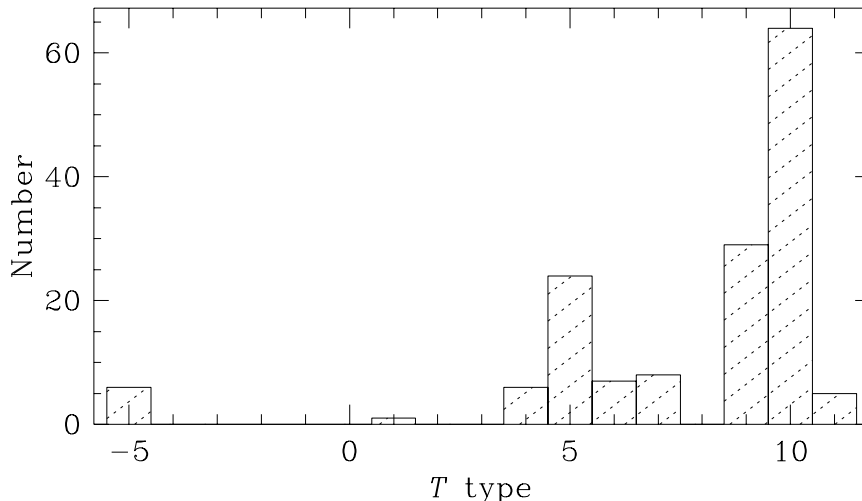


Figure 5: Histogram of T -types for LSB galaxies from the APM survey. Galaxies that appeared to be spirals but whose images on the APM scans were too small to permit reliable further classification were assigned $T = 5$, so the number in that bin is somewhat inflated. Interacting galaxies were assigned $T = 11$.

As is obvious from Figure 4, the maximum likelihood Schechter function is a very poor representation of the “true” distribution as determined by the SWML method: the reduced χ^2_ν from the likelihood ratio test of Efstathiou et al. (1988) is 14.04, which implies that the probability of exceeding this χ^2_ν by chance is $\sim 2.5 \times 10^{-18}$. The Schechter function is particularly poor at the low-luminosity end. There, the model-independent SWML method finds two to three times the galaxy density predicted by the maximum likelihood Schechter function. The SWML bins at $M = -16, -15, -14,$ and -13 contain 31, 9, 15, and 12 galaxies respectively. Across those four bins, the median correction due to the APM selection function (Paper II) is 0.759, and the median correction due to the incomplete spectroscopic observations (Equations 3 and 2) is 0.259; the median total incompleteness correction (Equation 4) is therefore 0.197. Our sampling of galaxies in these low-luminosity bins is quite sparse, and hence the uncertainties at this end are large. The formal uncertainties shown in Figure 4 may well understate the true range.

The dashed line in Figure 4 represents the Schechter function estimated by Marzke et al. (1994a) for all galaxy morphologies in the CfA Redshift Survey. At the faintest luminosities, LSB galaxies in the range $22.0 \leq \mu(0) \leq 25.0$ are more numerous than the HSB galaxies sampled by the CfA Survey if the comparison is based on the model-independent SWML points for the LSB galaxies, or approximately as numerous if the comparison is based on the maximum likelihood Schechter function. For all galaxies brighter than $M_B < -15$ the HSB galaxies are significantly more numerous. Table 1 lists the maximum likelihood Schechter function parameters for the LSB galaxies in the present study, along with similar parameters for all morphological types and for irregular galaxies from the CfA Survey.

The LSB sample from the APM survey is not restricted as to morphological type. It includes a few dwarf ellipticals and early spiral types. However, it is dominated by very late-type spirals and irregulars. As Figure 5 shows, over half the LSB sample have de Vaucouleurs T -types of 9 or 10. For that reason, we have also shown the Schechter function derived by Marzke et al. (1994a) for irregulars (which they define as $8 \leq T \leq 10$) in Figure 4 and Table 1. The Schechter function for the CfA irregulars bears a striking resemblance to that derived here for the LSB galaxies. The steep low luminosity tail of the function for CfA irregulars seems to match the model independent SWML points for the LSB galaxies quite well. This similarity in LF slopes could be used as an argument that the high space density of star forming irregulars are the parent population of the fainter LSBs. Unfortunately, photometric surveys of LSBs continue to find no relation between SB and color which is required to support such a fading model.

Table 1: Comparison of Luminosity Function Model Parameters

Model/Survey (1)	α (2)	M^* (3)	ϕ^* (4)
Maximum-Likelihood Schechter Functions:			
LSB	-1.46	-18.66	0.0036
CfA (all types)	-1.02	-18.90	0.0201
CfA (Sm - Im)	-1.87	-18.79	0.0006
Schechter Function + Power Law:			
LSB (giants)	-0.92	-18.19	0.0060
LSB (dwarfs)	-2.20	-16.00	0.0041

Notes: M^* in B mag, ϕ^* in $h_{100}^3 \text{Mpc}^{-3} \text{mag}^{-1}$.

Several authors have suggested that the LF for faint galaxies may exhibit an upturn from the pure Schechter form at faint luminosities. The LF of Impey et al. (1988) for LSB dE's in the Virgo cluster turns up at an apparent magnitude $m_B = 17$; the increase is so steep that they were unable to rule out a divergent faint-end slope (i.e., $\alpha = -2.0$). Upturns from the Schechter form have been observed in Coma by Thompson & Gregory (1993); in nearby local groups by Ferguson & Sandage (1991); in four local Abell clusters by De Propris et al. (1995); and in Coma, Abell 2554 and Abell 963 by Driver & Phillipps (1996). These deviations from the Schechter form are generally seen to begin in the range $-17 \leq M_B \leq -15$, after adjustment to the distance scale used here ($H_0 = 100 h_{100} \text{ km s}^{-1} \text{ Mpc}^{-1}$). In contrast, Ferguson & Sandage (1988) found an LF for the Fornax cluster that was consistent with a single Schechter function having a faint-end slope of $\alpha = -1.34$. We note that the form of

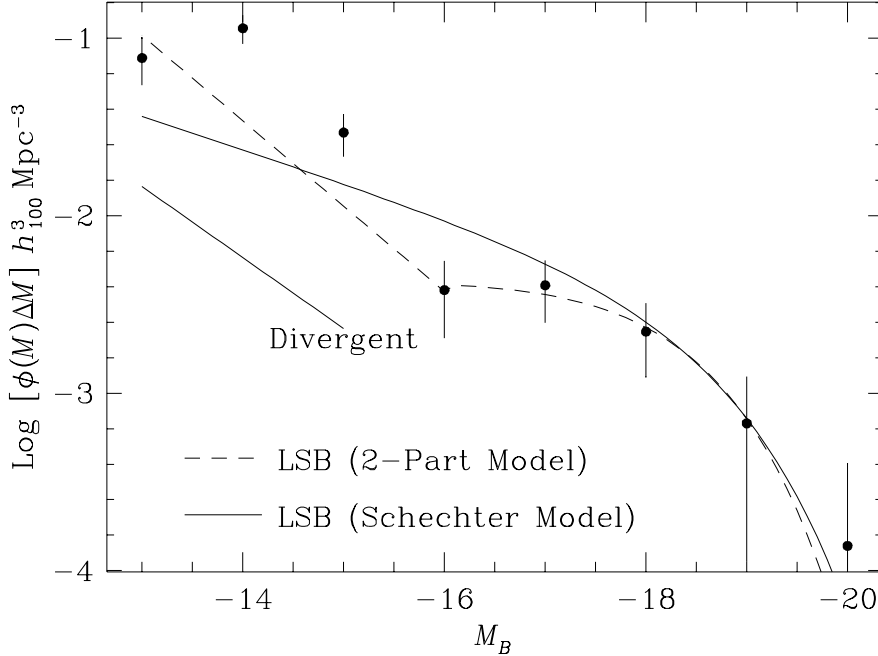


Figure 6: Luminosity function for LSB galaxies from the APM survey, determined using the two-component model described in the text (dashed curve), and maximum likelihood Schechter function (solid curve). The points with error bars represent the model-independent step-wise maximum likelihood LF. For galaxies brighter than $M = -16$ the two-component model is a standard Schechter function with all three parameters allowed to vary. For galaxies fainter than $M = -16$, the model is a power law with the normalization at $M = -16$ constrained to match the value of the Schechter component there. Note that this model was fit to the SWML binned LF, and not to the individual galaxy data points. The fiducial line labeled “Divergent” illustrates the faint end slope $\alpha = -2$ where the integral of the LF becomes divergent.

the SWML data points in Figure 4 is consistent with earlier findings of a sharp change in slope at faint luminosities: the binned model-independent data points clearly break up from a smooth Schechter form at $M = -16$.

To investigate this break in more detail, we also fit a two-component model to the SWML LF representation. For absolute magnitudes $M \leq -16$ (“giants”), the model followed the usual Schechter function form, with all three parameters (α , M^* , and ϕ^*) allowed to vary. For absolute magnitudes $M \geq -16$ (“dwarfs”), the model followed a simple power law, with the normalization at $M = -16$ constrained to match the Schechter model value there (i.e., only the slope α was allowed to vary in the fit). Results of this fit are depicted in Figure 6, and the fitted model parameters are listed in Table 1. Two aspects of this fit deserve special comment. First, it is not possible to compare directly the goodness-of-fit of this two-component model to that of the STY maximum-likelihood Schechter function. The

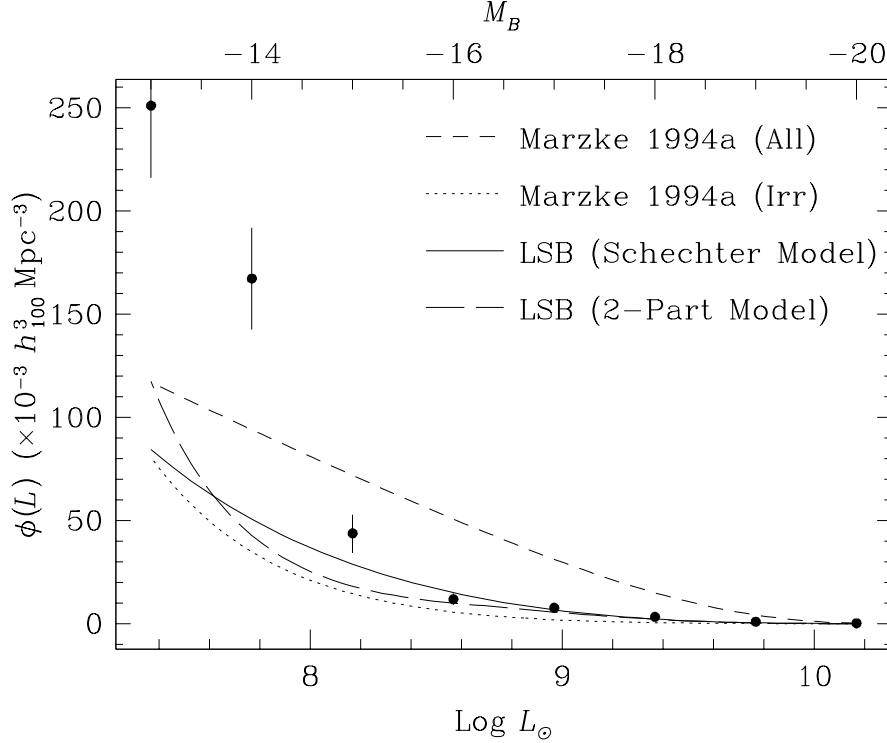


Figure 7: Cumulative luminosity functions for LSB galaxies and for galaxies from the CfA redshift survey, plotted linearly as a function of $\text{Log } L$. The top axis represents the corresponding B magnitude. The cumulation runs from high to low luminosities (i.e., from right to left). The points represent the binned model independent LF for the LSB galaxies, the solid line represents the maximum likelihood Schechter function for the LSB galaxies, and the long-dashed line represents the two-component model LF for the LSB galaxies. The short-dashed line is the Schechter function determined by Marzke et al. (1994) for all morphological types in the CfA redshift survey, and the dotted line is the Schechter function determined by Marzke et al. (1994) for irregulars.

χ_ν^2 quoted above for the STY result is obtained by a likelihood-ratio test which, like the STY model itself, is computed from the individual galaxy data points. The two-component model is a fit to the binned SWML LF, not to the individual galaxy data points, and thus its much larger χ_ν^2 ($\chi_\nu^2 = 294.8$, due to the much smaller number of degrees of freedom) is computed in a very different manner. Second, the two-component model yields results which are not physically plausible. The resulting slope of the dwarf galaxy power law is $\alpha = -2.20$, which implies an infinite total luminosity if the two-component LF is integrated from zero to infinity. This faint-end slope is best interpreted as a finding that the model-independent SWML indicates a very steeply increasing density of faint galaxies, so steep in fact that a divergent LF cannot be ruled out (cf. Impey, Bothun & Malin 1988).

Because the low luminosity tail of the LSB luminosity function rises so steeply, the

contribution of LSB galaxies to the overall number density of field galaxies locally is quite large. Figure 7 shows the same luminosity functions as Figure 4 along with the two-component LF described above, but cumulated to show total number densities. The cumulation runs from high to low luminosities (i.e., from right to left), and the vertical axis scaling is linear. Across the whole range of luminosities, the LSB galaxies are almost twice as numerous as all the HSB galaxies in the CfA survey if the comparison is based on the SWML points for the LSB galaxies, or half as numerous if the comparison is based on the maximum likelihood Schechter function. Thus, even under the most conservative estimate, surveys like the CfA redshift survey have missed at least one-third of the local galaxy population due to surface brightness selection biases. The true missed fraction is almost certainly higher, even by the most conservative estimator. The LSB LF presented here covers only the range $22.0 < \mu(0) \lesssim 25.0$, but as McGaugh et al. (1995a) and Paper II showed, the distribution appears flat for SB levels $\mu(0) \geq 25.0$. Thus, surveys sensitive to fainter SB levels should find even higher number densities of galaxies.

Despite the significance of their total numbers, LSB galaxies contribute little to the total luminosity density of the local universe, because the highest number densities of LSB galaxies occur at the lowest galaxy luminosities. Figure 8 shows the cumulative luminosity densities for LSB galaxies from the APM survey and HSB galaxies from the CfA redshift survey. Again, the cumulation runs from high to low luminosities (right to left) and the vertical scaling is linear. By any estimator, LSB galaxies represent a small fraction of the total luminosity emitted by HSB galaxies from the CfA survey.

5 Implications

Much attention has been devoted over the past 15 years to the population of faint blue galaxies revealed in surveys sensitive to extended objects as faint as $m_{B_J} \sim 27$. These galaxies become bluer at fainter apparent magnitudes (Lilly et al. 1995). They generally are not at extreme redshifts: Lilly et al. (1995) found a median redshift of $z_{med} \approx 0.56$ for a sample of galaxies in the magnitude range $17.5 < I_{AB} < 22.5$. These galaxies are clustered more weakly than are most local bright galaxies, though their clustering strength is roughly comparable to that of local galaxies undergoing rapid star formation, per Bernstein et al. (1994). Their numbers are significantly in excess of expectations based on local galaxy populations in the absence of evolution (Tyson 1988; Lilly et al. 1991; McLeod & Rieke 1995). This excess has led some authors to suggest non-standard cosmologies as a possible explanation (Yoshii 1993), and others to propose strong evolution in galaxy luminosities, perhaps with the rate of evolution itself a function of luminosity (Broadhurst et al. 1988; Babul & Rees 1992; Babul & Ferguson 1996). Still another approach, taken by Gronwall & Koo (1995), is to derive local luminosity functions by finding functions that can explain as well as possible the faint galaxy number counts without invoking strong evolution. The

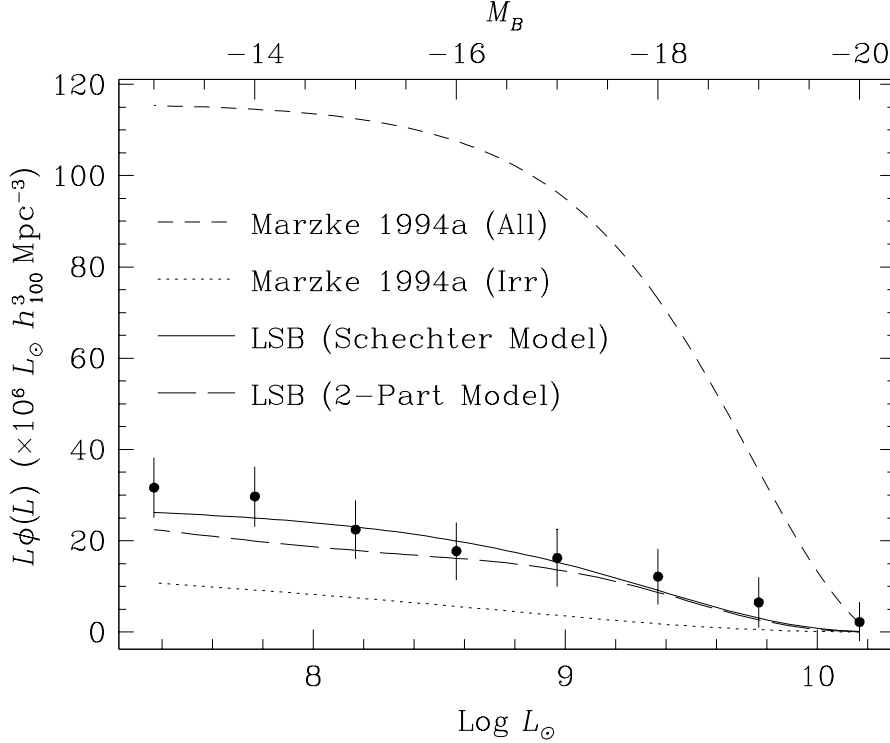


Figure 8: Cumulative luminosity densities for LSB galaxies and for galaxies from the CfA redshift survey, plotted linearly as a function of $\text{Log } L$. The top axis indicates the corresponding B magnitude. The points represent the binned model independent LF for the LSB galaxies, the solid represents the maximum likelihood Schechter function for the LSB galaxies, and the long-dashed line represents the two-component model LF for the LSB galaxies. The short-dashed line is the Schechter function for all morphological types in the CfA redshift survey determined by Marzke et al. (1994) and the dotted line is the Schechter function determined by Marzke et al. (1994) for irregulars. The cumulation runs from high to low luminosities (i.e., from right to left).

luminosity functions they derive predict more local low-luminosity galaxies than are observed in existing surveys. At the very least, recent surveys for LSB galaxies indicate that the galaxy density at $z = 0$ is higher than previously assumed which means, at some level, the apparent excess of faint galaxies at high redshifts is at least in part an artifact of improper normalization at $z = 0$. The issue is how large this effect really is.

McGaugh (1994) suggested that LSB galaxies such as those in the present sample could help reconcile the differences between observed local populations and this population of faint blue galaxies (hereafter, FBGs). He noted that, like the FBGs, LSB galaxies are generally blue (McGaugh & Bothun 1994) and weakly clustered (Mo et al. 1994). Furthermore, if current models of slow, continuous star formation LSB galaxies are correct (McGaugh & Bothun 1994), McGaugh (1994) argued that LSB galaxies should become only slightly redder

over the timescales of interest, $0 < z \lesssim 0.5$. He also demonstrated through a simple analytic calculation that the deep CCD surveys would be more sensitive to LSB galaxies at $z \sim 0.4$ than wide-field photographic surveys are to local ($z \lesssim 0.1$) LSB galaxies. He argued that including nearby LSB galaxies in the local luminosity function could reconcile the number of low-luminosity galaxies in the local population with the FBG population.

More recently still, Driver et al. (1995b) and Driver et al. (1995a) have examined the morphological mix of the faint field galaxies using data from the Hubble Space Telescope, down to a flux limit of $m_I = 24.25$. They compared the observed differential number counts (number per square degree as a function of apparent magnitude) for three different morphological groupings to the predictions of various models. They concluded that differential number counts of ellipticals and early-type spirals are consistent with the predictions of a no-evolution model based on standard local LFs (after renormalization) for these types taken from Marzke et al. (1994a) and Loveday et al. (1992). They also found that the observed number counts of late-type spirals and irregulars were substantially in excess of similar no-evolution predictions for these classes. They could reconcile prediction with observation for this morphological class only by including a substantial amount of luminosity evolution (1.3 magnitudes of brightening by $z \sim 0.5$ for an Irr LF from Marzke et al. (1994)) or by using a sharply increased normalization ($\phi^* = 3.5 \times 10^{-2} h_{100}^3 \text{Mpc}^{-3}$; compare with Table 1) for the Irr LF.

Our results underscore the uncertainty in the faint end slope of the field galaxy luminosity function. Driver & Phillipps (1996) have shown that existing wide field redshift surveys place few constraints on the shape of the luminosity function below $M_B = -16.5$ assuming $H_0 = 100 h_{100} \text{ km s}^{-1} \text{ Mpc}^{-1}$. By reaching lower in surface brightness, we have isolated a population of blue, LSB dwarfs that is absent from published luminosity functions, and which contributes strongly below $M_B = -16$. Marzke et al. (1994a) also saw evidence for a sharp upturn in the dwarf and irregular population at about the same luminosity. More recently, Zucca & et al. (1996) have shown that the luminosity function of Loveday et al. (1992) calculated from the Stromlo-APM survey is significantly incomplete. The new ESO Slice luminosity function shows an upturn below $M_B = -16$, due to blue, star-forming galaxies, made up of a mixture of compact dwarfs and LSB galaxies. In all these studies, as in the deeper HST surveys of Driver et al. (1995a), the data are well described by a hybrid luminosity function consisting of a bright end Schechter function with $\alpha = -1$, and a faint end ($M_B \gtrsim -16$ assuming $H_0 = 100 h_{100} \text{ km s}^{-1} \text{ Mpc}^{-1}$) power law with a slope $-1.4 < \alpha < -1.8$. These faint galaxies are not major contributors to the luminosity density of the universe, but because the trend of M/L with luminosity is not well understood their contribution to the mass density is an open issue.

There is also now evidence that some evolution may have occurred in the late-type galaxy population over the range $0 \leq z \leq 1$. Lilly et al. (1995) have studied the evolution of the LFs over this range using data from the recent Canada-France Redshift Survey (CFRS). They found that the LF for red galaxies shows little change in number density or luminosity

over this range in z , but that the LF for blue galaxies appears to have brightened uniformly by about 1 magnitude by $z \sim 0.75$.

Thus, the “excess” of FBGs consists of late-type spirals and irregulars, the same types which dominate the population of LSB galaxies found by the APM survey (Fig 5). These LSB galaxies have a Schechter function normalization approximately 6 times as large as that found by Marzke et al. (1994a) for HSB irregulars, so they expand the known local population well beyond that used by Driver et al. (1995b) in their modeling. The LSB normalization still is not as large as that found necessary by Driver et al. (1995b) to account for the FBG counts with no evolution, but the heretofore-unaccounted LSB galaxies do help considerably to close the gap between local population estimates and the FBG counts. Taking this increase together with the modest evolution observed in blue galaxy LFs by Lilly et al. (1995), it may now be possible to make an essentially complete reconciliation between local populations and the FBGs. However, any such reconciliation will also require a model for the evolution of the FBGs which accounts for the very blue colors of both the FBGs and the local LSBs (see McGaugh & Bothun 1994, McGaugh 1994, and McGaugh et al. 1995a).

We can demonstrate the rough equivalence between the local LSB dwarf population and the MDS population of Driver et al. (1995a), which we presume to be at typical redshifts $0.3 \lesssim z \lesssim 0.6$ based on Lilly et al. (1995). The LSB dwarfs with $M_B > -16$ are at typical distances of $10 \lesssim d \lesssim 40 h_{100}^{-1}$ Mpc. They have central surface brightness in the range $22.0 < \mu_B(0) \lesssim 25$ mag arcsec $^{-2}$, and effective angular radii of $6 \lesssim r_{eff} \lesssim 20$ arcseconds. If they are related to the LSB dwarfs in clusters, we expect them to have $B-V \sim 0.5$ (Impey, Bothun, & Malin 1988). The late-type and irregular (Sdm/Irr) MDS galaxies have effective radii with a median value of 0.4 arcseconds (Im et al. 1995), which would scale to $20 \lesssim r_{eff} \lesssim 40$ arcseconds for a local population. The central surface brightnesses of disk-dominated categories in the MDS sample are $20 \lesssim \mu_I(0) \lesssim 22$ mag arcsec $^{-2}$ per Mutz et al. (1994), which is equivalent to $22 \lesssim \mu_B(0) \lesssim 24$ mag arcsec $^{-2}$ locally, assuming no evolution. The Sdm/Irr galaxies have observed colors of $V-I \sim 1$ per Casertano et al. (1995), consistent with a local star-forming dwarf color of $B-V \sim 0.5$, once again assuming no evolution. There could well be a subset of the MDS population which fade in surface brightness and redden to below the detection threshold for our blue photographic survey. Such galaxies would be absent from all local catalogs.

6 Conclusions

We have estimated a luminosity function for galaxies with surface brightnesses fainter than $\mu(0) = 22.0$ mag arcsec $^{-2}$, which is the approximate faint limit of $\mu(0)$ for galaxies covered by the CfA Redshift Survey. We find that this LSB LF has a steeply rising tail at low luminosities ($\alpha = 1.42$), comparable to that found by Marzke et al. (1994a) for galaxy types $8 \leq T \leq 10$. The LSB LF has a normalization lower than that found for the overall CfA

survey, but much higher than that found for types $8 \leq T \leq 10$. Thus estimates of the total population of local galaxies based on the CfA survey are missing at least one-third of the total number of galaxies due to surface brightness selection bias. These previously unaccounted-for LSB galaxies can help considerably to resolve the apparent difference between estimates of the local population and the large numbers of faint blue galaxies observed at moderate redshift.

We are grateful to a number of our colleagues for many stimulating and helpful discussions. We thank in particular: Frank Briggs, Erwin de Blok, Simon Driver, Marijn Franx, Ron Marzke, Stacy McGaugh, Renzo Sancisi and Martin Zwaan. We also thank the staffs of the Multiple Mirror Telescope Observatory, the Steward Observatory Kitt Peak Station, and the Arecibo Observatory for their expert assistance during the many observing runs carried out in connection with our survey. This project made extensive use of the NASA Astrophysics Data System. This work was supported in part by the National Science Foundation under Grant AST-9003158.

REFERENCES

- Babul, A. & Ferguson, H. C. 1996, *ApJ*, 458, 100
- Babul, A. & Rees, M. J. 1992, *MNRAS*, 255, 346
- Bernstein, G. M., Tyson, J. A., Brown, W. R., & Jarvis, J. F. 1994, *ApJ*, 426, 516
- Binggeli, B., Sandage, A., & Tammann, G. A. 1988, *ARA&A*, 26, 509
- Bothun, G. D. & Cornell, M. E. 1990, *AJ*, 99, 1004
- Bothun, G. D., Impey, C. D., & Malin, D. F. 1991, *ApJ*, 376, 404
- Broadhurst, T. J., Ellis, R. S., & Shanks, T. 1988, *MNRAS*, 235, 827
- Casertano, S., Ratnatunga, K. U., Griffiths, R. E., Im, M., Neuschaefer, L. W., Ostrander, E. J., & Windhorst, R. A. 1995, *ApJ*, 453, 599
- Coleman, G. D., Wu, C.-C., & Weedman, D. W. 1980, *ApJS*, 43, 393
- Davis, M. & Huchra, J. 1982, *ApJ*, 254, 437
- De Propris, R., Pritchet, C. J., Harris, W. E., & McClure, R. D. 1995, *ApJ*, 450, 534
- Disney, M. & Phillipps, S. 1983, *MNRAS*, 205, 1253
- Disney, M. J. 1976, *Nature*, 263, 573
- Driver, S. P. & Phillipps, S. 1996, *ApJ*, 469, 529
- Driver, S. P., Windhorst, R. A., & Griffiths, R. E. 1995a, *ApJ*, 453, 48
- Driver, S. P., Windhorst, R. A., Ostrander, E. J., Keel, W. C., Griffiths, R. E., & Ratnatunga, K. U. 1995b, *ApJ*, 449, L23
- Efstathiou, G., Ellis, R. S., & Peterson, B. A. 1988, *MNRAS*, 232, 431, (EEP)
- Ferguson, H. C. & McGaugh, S. S. 1995, *ApJ*, 440, 470
- Ferguson, H. C. & Sandage, A. 1988, *AJ*, 96, 1520
- Ferguson, H. C. & Sandage, A. 1991, *AJ*, 101, 765
- Freeman, K. C. 1970, *ApJ*, 160, 811
- G., B. A. & Kron, R. G. 1980, *ApJ*, 241, 25
- Gronwall, C. & Koo, D. C. 1995, *ApJ*, 440, L1

- Guiderdoni, B. & Rocca-Volmerange, B. 1990, *A&A*, 227, 362
- Hall, P. & Mackay, C. D. 1984, *MNRAS*, 210, 979
- Im, M., Casertano, S., Griffiths, R. E., Ratnatunga, K. U., & Tyson, J. A. 1995, *ApJ*, 441, 494
- Impey, C., Bothun, G., & Malin, D. 1988, *ApJ*, 330, 634
- Impey, C. D., Sprayberry, D., Irwin, M. J., & Bothun, G. D. 1996, *ApJS*, 105, 209
- Irwin, M. J., Davies, J. I., Disney, M. J., & Phillipps, S. 1990, *MNRAS*, 245, 289
- Kibblewhite, E. J., Bridgeland, M. T., Bunclark, P. S., & Irwin, M. J. 1984, in *NASA Conf. Pub. No. 2317, Astronomical Microdensitometry Conference*, ed. D. A. Klinglesmith, (Washington, D. C.: NASA), 277
- Koo, D. C., Gronwall, C., & Bruzual A., G. 1993, *ApJ*, 415, L21
- Kron, R. G. 1980, *ApJS*, 43, 305
- Lilly, S. J., Cowie, L. L., & Gardner, J. P. 1991, *ApJ*, 369, 79
- Lilly, S. J., Tresse, L., Hammer, F., Crampton, D., & Le Fevre, O. 1995, *ApJ*, 455, 108
- Loveday, J., Peterson, B. A., Efstathiou, G., & Maddox, S. J. 1992, *ApJ*, 390, 338
- Marzke, R. O., Geller, M. J., Huchra, J. P., & Corwin, Jr., H. G. 1994a, *AJ*, 108, 437
- Marzke, R. O., Huchra, J. P., & Geller, M. J. 1994b, *ApJ*, 428, 43
- McGaugh, S. S. 1994, *Nature*, 367, 538
- McGaugh, S. S. & Bothun, G. D. 1994, *AJ*, 107, 530
- McGaugh, S. S., Bothun, G. D., & Schombert, J. M. 1995a, *AJ*, 110, 573
- McGaugh, S. S., Schombert, J. M., & Bothun, G. D. 1995b, *AJ*, 109, 2019
- McLeod, B. A. 1994, Ph.D. thesis, Univ. of Arizona
- McLeod, B. A. & Rieke, M. J. 1995, *ApJ*, 454, 611
- Mo, H., McGaugh, S. S., & Bothun, G. D. 1994, *MNRAS*, 267, 129
- Mutz, S. B., Windhorst, R. A., Schmidtke, P. C., Pasacarelle, S. M., Griffiths, R. E., Ratnatunga, K., Im, M., & Neuschaefer, L. W. 1994, *ApJ*, 434, L55
- Phillipps, S., Davies, J. I., & Disney, M. J. 1990, *MNRAS*, 242, 235

- Press, W. P. & Schechter, P. 1974, ApJ, 187, 425
- Sandage, A., Tammann, G. A., & Yahil, A. 1979, ApJ, 232, 352, (STY)
- Schechter, P. 1976, ApJ, 203, 297
- Schmidt, M. 1968, ApJ, 151, 393
- Sprayberry, D., Impey, C. D., & Irwin, M. J. 1996, ApJ, 463, 535
- Thompson, L. A. & Gregory, S. A. 1993, AJ, 106, 2197
- Tyson, J. A. 1988, AJ, 96, 1
- Yoshii, Y. 1993, ApJ, 403, 552
- Zucca, E. & et al. 1996, in 37th Herstmonceaux Conference, HST and The High Redshift Universe, ed. M. Pettini, (Cambridge: Cambridge Univ. Press), (in press)
- Zucca, E., Pozzetti, L., & Zamorani, G. 1994, MNRAS, 269, 953